Expression and distribution of sodium channels in short- and long-term denervated rodent skeletal muscles

M. T. Lupa, D. M. Krzemien, K. L. Schaller and J. H. Caldwell*

University of Colorado Health Sciences Center, Departments of Cellular and Structural Biology and Physiology and the Neuroscience Program, B-111, 4200 E. 9th Avenue, Denver, CO 80262, USA

1. Loose-patch voltage-clamp recordings were made from rat and mouse skeletal muscle fibres denervated for up to 6 weeks. Innervated muscles possessed a Na^+ current density of $107 \pm 3{\cdot}3$ mA cm^{-2} in endplate membrane, and $6{\cdot}3 \pm 0{\cdot}6$ mA cm^{-2} in extrajunctional membrane. This high concentration of Na^+ channels at the endplate was gradually reduced following denervation. After 6 weeks of denervation, the endplate Na^+ channel concentration was reduced by 40–50%, and the density of Na^+ channels in extrajunctional membrane was increased by about 30%.

2. The tetrodotoxin (TTX)-resistant form of the Na^+ channel appeared after 3 days of denervation and comprised ~43% of the endplate Na^+ channels 5–6 days after denervation. Subsequently, TTX-resistant Na^+ channels were reduced in density to ~25% of the postjunctional Na^+ channels and remained at this level up to 6 weeks after denervation.

3. RNase protection analysis showed that mRNA encoding the TTX-resistant Na^+ channel was virtually absent in innervated muscle, rose > 50-fold after 3 days of denervation, then decreased by 95% 6 weeks after denervation. The density of TTX-resistant Na^+ channels correlated qualitatively with changes in mRNA levels.

4. These results suggest that the density of Na^+ channels at neuromuscular junctions is maintained by two mechanisms, one influenced by the nerve terminal and the other independent of innervation.

Innervation has been shown to affect many properties of skeletal muscle fibres. These include mRNA and protein expression, membrane properties and synaptic function. We have been investigating the regulation of one synaptic specialization, the concentration of voltage-activated Na^+ channels in the postsynaptic membrane (Betz, Caldwell & Kinnamon, 1984; Beam, Caldwell & Campbell, 1985; Caldwell, Campbell & Beam, 1986). It has been previously shown that the high density of Na^+ channels is maintained at mammalian endplates up to 14 days after denervation (Caldwell & Milton, 1988). Since the density of acetylcholine receptors (AChRs) has been found to be diminished at endplates denervated for longer than 3 weeks (Frank, Gautvik & Sommerschild, 1975; Fumagalli, Balbi, Cangiano & Lømo, 1990), we decided to use the loose-patch voltage-clamp technique to study whether long-term denervation affects the distribution of Na^+ channels in the muscle cell membrane. We found that the density of Na^+ channels is reduced by about 40% at endplates denervated for 6 weeks, while the extrajunctional density of Na^+ channels is increased by approximately 30%.

Denervation also induces the reappearance of an embryonic form of the Na^+ channel, one that is relatively resistant to the blocking action of tetrodotoxin (TTX). The abundance of TTX-resistant Na^+ current in the muscle membrane reaches a peak after 3–5 days of denervation and declines thereafter up to 21 days following denervation (Sellin & Thesleff, 1980). It appeared possible that the expression of TTX-resistant Na^+ channels could be a temporary response that disappears after long-term denervation, and that this might be a mechanism by which the endplate Na^+ channel concentration could become reduced after long-term denervation. To answer this question we have used RNase protection analysis and loose-patch voltage clamp to compare the regulation of Na^+ channel mRNA and protein isoforms in denervated muscle.

* To whom correspondence should be addressed.

METHODS

Muscle preparation

The lower leg and foot muscles, including the flexor digitorum brevis (FDB) muscle, were denervated by transecting the sciatic nerve in mid-thigh under ether anaesthesia. For long-term denervation this procedure was repeated every 2 weeks for mice, every 3 weeks for rats. The continuity of denervation was confirmed by the absence of a toe-spreading reflex before killing the animal and by the absence of a twitch elicited through stimulation of the nerve stump *in vitro*.

FDB muscles were taken from adult (4- to 12-month-old) C57BL6 mice or Sprague–Dawley rats after an overdose of ether. Muscles were enzymatically dissociated into single fibres as previously described (Lupa & Caldwell, 1991). The physiological saline solution contained (mM): NaCl, 146; KCl, 5; $CaCl_2$, 2; $MgCl_2$, 1; glucose, 11; Na_2Pipes, 2; with a pH of 7·3. Muscle fibres were labelled with 50 nM rhodamine-conjugated α-bungarotoxin (α-BuTX) to visualize AChRs and viewed on an inverted Nikon Diaphot microscope equipped with Hoffman modulation contrast and epifluorescence optics. Images were captured digitally by an SIT camera coupled to a Silicon Graphics Iris computer and analysed with a software package from G. W. Hannaway (Boulder, CO, USA) as described in Lupa & Caldwell (1991).

Loose-patch voltage clamp

Loose-patch voltage-clamp recording (Strickholm, 1961; Stühmer & Almers, 1982) was done as previously described (Lupa & Caldwell, 1991). Electrode tip diameters were 6–17 μm, and a steady hyperpolarizing potential of 70 mV was applied to the patch for 2–3 min before recording in order to remove slow inactivation of Na^+ channels (Almers, Stanfield & Stühmer, 1983). Depolarizing pulses of 4 ms duration and different voltage steps were applied to obtain maximum inward current (the voltage step which produced the maximum current is shown in Fig. 1). These currents were then normalized and converted to current density measurements by assuming that the area of membrane under voltage clamp was equal to the area under the tip of the pipette (see Lupa,

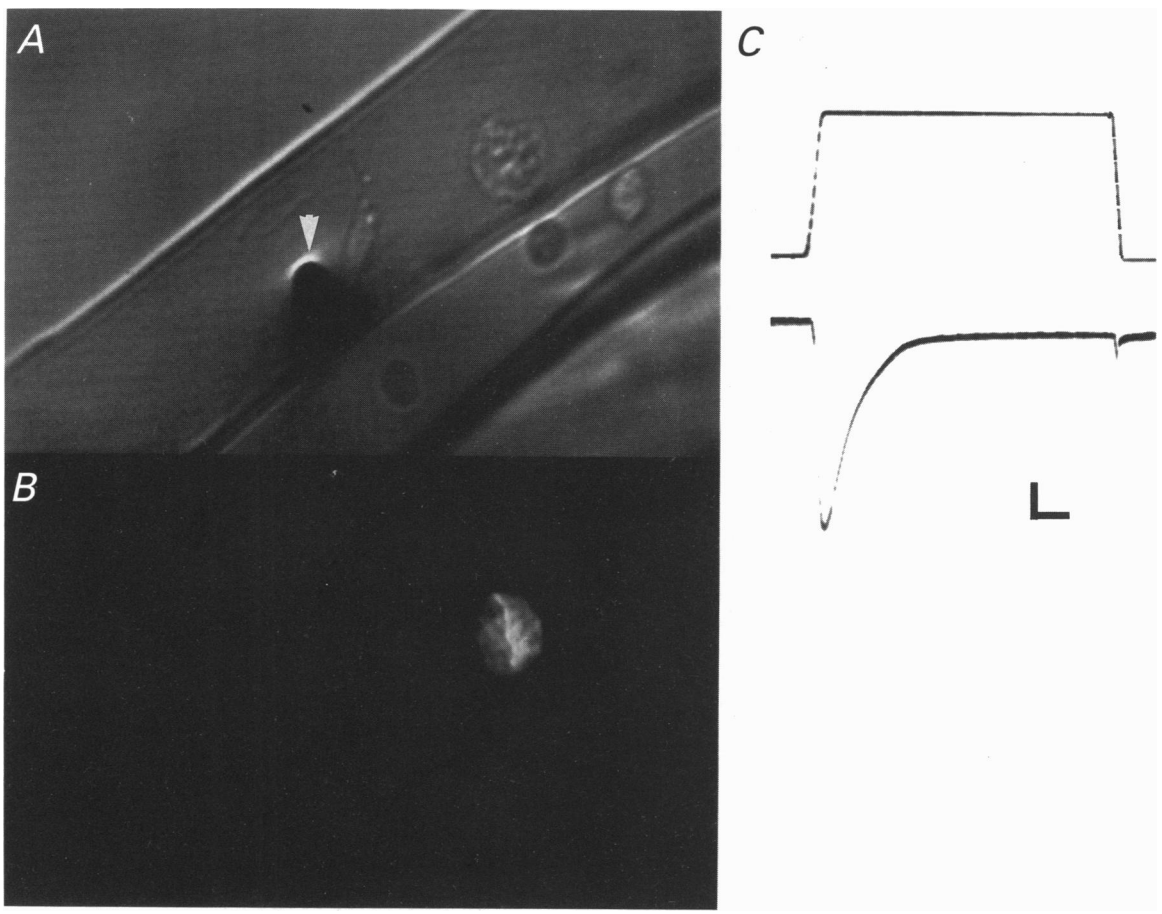

Figure 1. Loose-patch clamp recording from enzymatically dissociated FDB muscle fibres

A, Hoffman modulation contrast photograph of a dissociated mouse FDB muscle fibre; the loose-patch electrode (arrowhead) is in position to record from a patch of extrajunctional membrane. *B*, a fluorescence micrograph showing α-BuTX labelling of the endplate on the muscle cell shown in *A*. *C*, recording of Na^+ current from the endplate on the muscle fibre. The top trace is the command voltage applied to the membrane patch. From a steady hyperpolarizing potential of −70 mV the membrane is depolarized 100 mV. The bottom trace shows the Na^+ current recorded during the pulse. The calibration bar (shown in *C*) is 20 mA cm^{-2} and 0·5 ms for *C* and 10 μm for *A* and *B*.

Krzemien, Schaller & Caldwell (1993) for discussion of this assumption).

For determination of TTX-resistant Na^+ currents, fibres were studied in normal physiological saline, and this saline was replaced twice with one containing 300 nM TTX. The solution inside the pipette was also exchanged in order to ensure a constant concentration of TTX at the patch. Fibres were relocated by use of a stage micrometer and photographs. By assuming a dissociation constant (K_d) of 1 μM for the TTX-resistant Na^+ channel and 10 nM for the TTX-sensitive Na^+ channel, one can calculate that 300 nM TTX will block about 97% of the TTX-sensitive channels, as well as 23% of the TTX-resistant channels. In order to obtain estimates of the population of TTX-sensitive and TTX-resistant Na^+ channels, we calculated corrected values for the true TTX-resistant current obtained in 300 nM TTX by applying the equation:

$$I_{Na,TTX} = \{I_{Na,TOX} - 0{\cdot}03(I_{Na,TOT})\}/0{\cdot}74,$$

where $I_{Na,TTX}$ is the corrected TTX-resistant Na^+ current density, $I_{Na,TOX}$ is the uncorrected current density recorded in 300 nM TTX, and $I_{Na,TOT}$ is the current density measured in normal saline solution.

RNase protection analysis

Quantitation of mRNA abundance for the TTX-resistant Na^+ channel was accomplished with RNase protection assays as previously described (Lupa *et al.* 1993). An antisense RNA probe for a portion of a cytoplasmic domain of the TTX-resistant Na^+ channel (nucleotides 4439–4844; Rogart, Cribbs, Muglia, Kephart & Kaiser, 1989) was produced using SP6 polymerase on linearized template (Melton, Krieg, Rebagliati, Maniatis, Zinn & Green, 1984) in the presence of ^{32}P-labelled cytidine triphosphate (CTP) (Amersham, UK). Total cellular RNA was isolated from rat FDB muscles and stored at −80 °C as a precipitate in guanidinium and isopropanol. Total RNA (30–40 μg) was hybridized to $1–2 \times 10^6$ c.p.m. of the cRNA probe in 50 μl hybridization buffer (40 mM Pipes (pH 6·4), 1 mM EDTA, 0·4 M NaCl, 80% formamide) overnight at 45 °C. Ribonucleases A (40 μg ml^{-1}) and T1 (2 μg ml^{-1}) were then added to digest unhybridized RNA; these were subsequently eliminated by addition of 35 μg proteinase K and a phenol–chloroform extraction. The protected RNA was ethanol precipitated for 1 h at −20 °C and washed once with 70% ethanol. The RNA was run on a 5% polyacrylamide, 7 M urea gel and exposed to Amersham Hyperfilm with an intensifying screen at −70 °C. Controls for non-specific binding included samples of rat liver RNA and yeast tRNA. No signals were obtained with these samples.

Quantitation was achieved by hybridizing known amounts of the sense strand to the corresponding Na^+ channel probe RNA. Autoradiographs were digitized with an image analysis system comprising an Apple Macintosh IIx processor with a Data Translation video capture card, a COHU video camera (model 4815-2000), and the NIH Image 1.43 analysis software (from the US National Technical Information Service). The automatic gain and black adjust controls in the camera were turned off to prevent the camera from adjusting for variations in light intensity between and within autoradiographs. Bands obtained with known amounts of the sense strand for the probe were used to generate a calibration curve. This curve was then applied automatically to all measurements taken from experimental lanes. The probe recognizing the mRNA for the TTX-resistant Na^+ channel isoform was fully protected by hybridization to the total RNA samples, producing a band corresponding to 405 nucleotides.

Statistics

Na^+ current density is given as means ± S.E.M. Regression analysis of data in Fig. 3 was based on a model (Laird & Ware, 1982) which allows the incorporation of a random subject effect. Virtually the same linear regression result was obtained using simple weighted and unweighted regression models. Significance in Fig. 4 was tested by Student's t test for unpaired parameters.

RESULTS

Denervation of the FDB muscle produced changes in the appearance of individual dissociated fibres (Fig. 2). After 2–3 weeks of denervation, the fibres became noticeably atrophied when compared with innervated fibres, and fibrillation was often observed. The endplate became difficult to identify without the aid of α-BuTX, although it could often be discerned as a local bulging of the sarcolemma (see also Matsuda, Oki, Kitaoka, Nagano, Nojima & Desaki, 1988). No obvious change in the pattern or appearance of the α-BuTX fluorescence was apparent, even after 6 weeks of denervation. Muscle fibres which had been denervated for 4–6 weeks sometimes exhibited clusters of AChRs in extrajunctional membrane (Fig. 2).

Endplate and extrajunctional Na^+ channel density

Na^+ channels are concentrated in the postjunctional membrane of mammalian skeletal muscles, where a Na^+ current density of about 100 mA cm^{-2} can be measured (Beam *et al.* 1985; Caldwell *et al.* 1986; Roberts, 1987). In order to examine the long-term stability of this synaptic specialization, we recorded Na^+ currents at endplates of muscle fibres denervated for as long as 6 weeks (Fig. 3). The Na^+ current density at the endplate was reduced after 6 weeks of denervation to $56{\cdot}0 \pm 3{\cdot}4$ mA cm^{-2}. This is similar to the approximately 50% reduction in AChR density at endplates denervated for 4–6 weeks (Frank *et al.* 1975; Fumagalli *et al.* 1990). Regression analysis indicated that the decrease in Na^+ current density with time could be fitted with a straight line of slope −1·08 (mA cm^{-2} day^{-1}) which is statistically significant ($P = 0{\cdot}0024$).

After denervation, there is a rapid expansion in the extent of sarcolemmal membrane that is sensitive to acetylcholine, due to an increase in AChR density in the extrajunctional membrane (Axelsson & Thesleff, 1959; Thesleff & Sellin, 1980). To test whether the density of Na^+ channels in extrajunctional membrane changed after long-term denervation, we mapped Na^+ current density along individual FDB fibres from innervated and 6-week-denervated muscles (Fig. 4). Two differences are evident in the maps. First, as described above, the current density at the endplate was reduced by long-term denervation to about 60% of the control level. Secondly, the density of Na^+ current in extrajunctional membrane of denervated

muscle was about 30% higher than in innervated muscle ($P < 0.05$). Because of these alterations, the density of Na^+ channels at the endplates of denervated muscle is only about 4- to 5-fold higher than in the extrajunctional membrane, compared with a 12-fold concentration found at innervated endplates. The area over which Na^+ channels were concentrated remained unchanged after denervation. The gradient in Na^+ channel density for distances greater than 25 μm from the endplate did not appear to change after denervation.

Expression of the TTX-resistant Na^+ channel isoform

In agreement with previous results (Redfern & Thesleff, 1971; Sellin, Libelius, Lundquist, Tågerud & Thesleff, 1980), TTX-resistant Na^+ current was first detected 3 days after denervation (Fig. 5). The percentage of TTX-resistant Na^+ current at the endplate increased rapidly over the next 2–3 days to approximately 43% of the total Na^+ current density. This percentage then fell to about 25% by 3 weeks following denervation. Although the total current

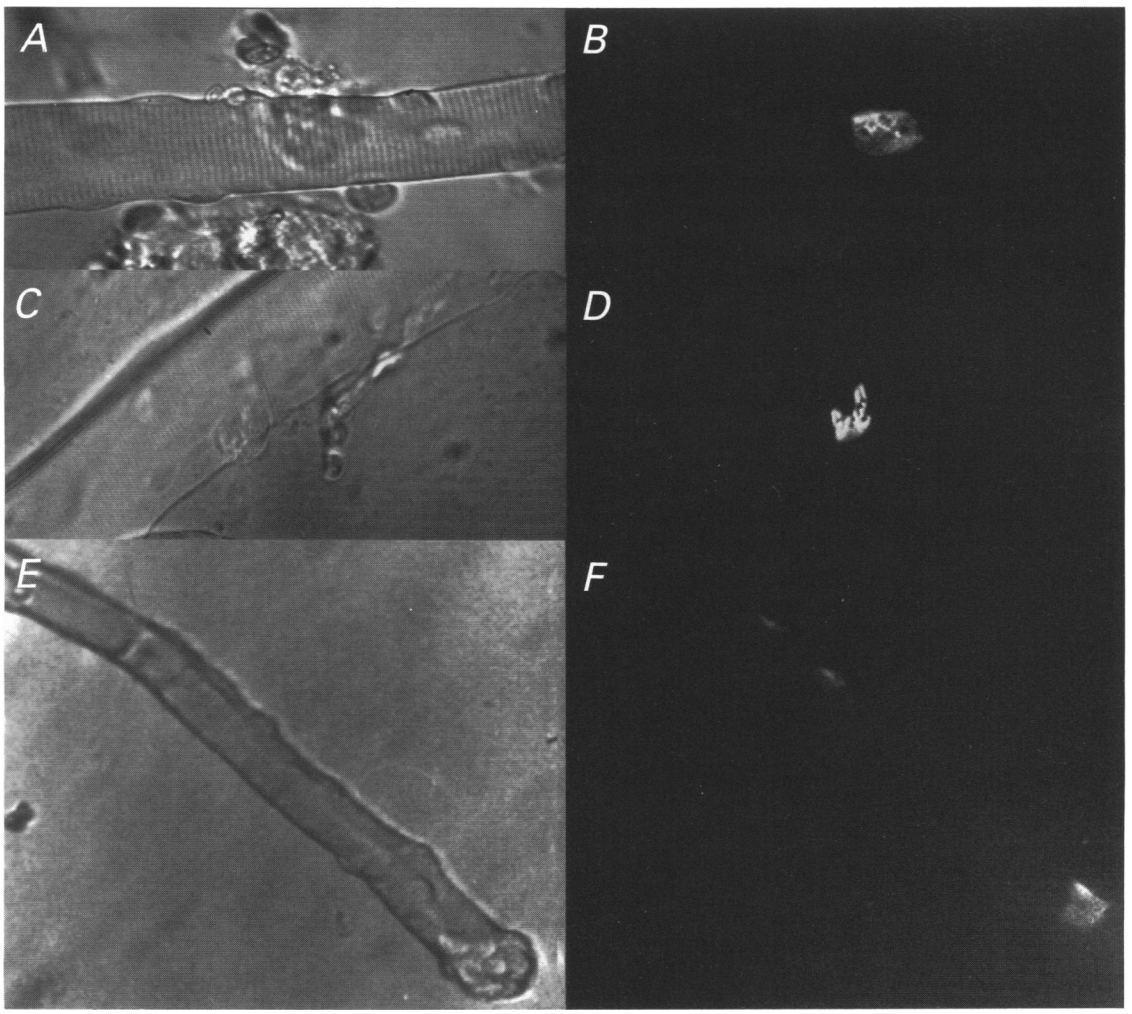

Figure 2. Examples of single muscle fibres enzymatically dissociated from rat FDB muscles at different times after denervation

Panels on the left (*A*, *C* and *E*) are taken with Hoffman modulation contrast optics. Panels on the right (*B*, *D* and *F*) are fluorescence micrographs showing AChRs labelled with α-BuTX. Top panels (*A* and *B*) are images from an innervated fibre; middle panels (*C* and *D*) are from a fibre denervated for 3 weeks, and bottom panels (*E* and *F*) are from a fibre denervated for 6 weeks. Note that the 6-week-denervated muscle fibre possessed extrajunctional clusters of AChRs. The endplate is near the tendon on this fibre (*E* and *F*), which is not uncommon for the short muscle fibres of the FDB. The fibre in *C* and *D* is larger than the average diameter of 3-week-denervated muscles. Fibre diameters are 37 μm (*A* and *B*), 53 μm (*C* and *D*) and 25 μm (*E* and *F*).

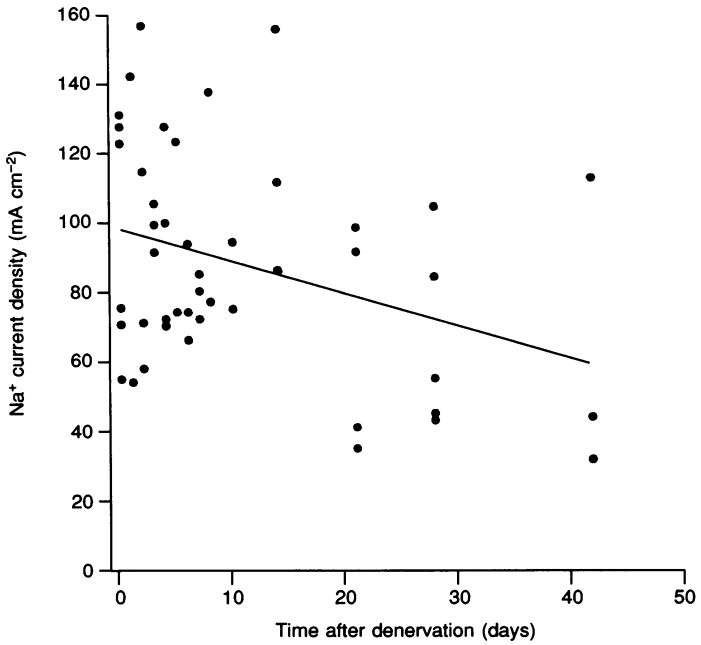

Figure 3. Na^+ current density (mA cm^{-2}) at neuromuscular endplates of innervated mouse FDB muscle fibres (day 0) and endplates that had been denervated for up to 6 weeks

Each data point is the average current density from one animal. The decrease in current density with time could be fitted with a straight line of slope −1·08.

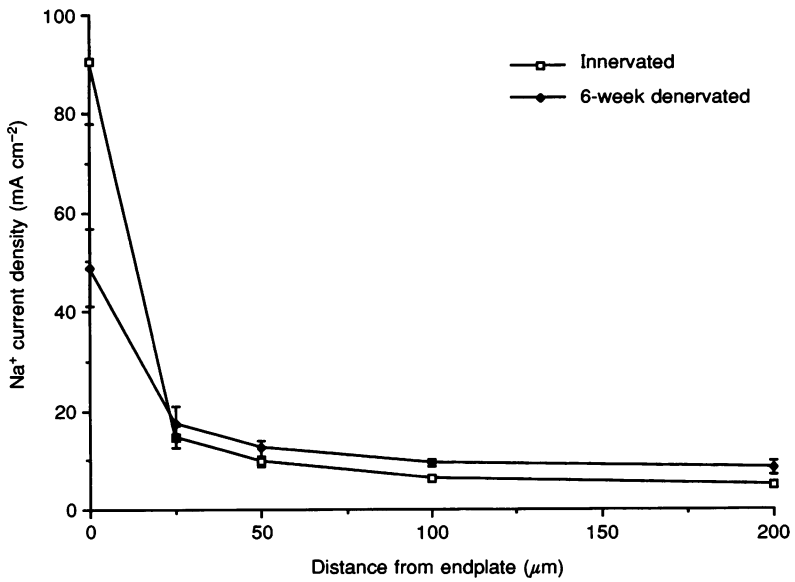

Figure 4. Na^+ current density on individual muscle fibres

Maps of Na^+ current density on innervated rat FDB muscle fibres (□) and on FDB fibres denervated for 6 weeks (◆). Each point represents the mean ± S.E.M. for 7–10 fibres.

density at the endplate became progressively reduced during 6 weeks of denervation (Figs. 3 and 4), the percentage of Na^+ current density resistant to TTX remained between 20 and 30% up to the end of the sixth week of denervation. Thus, after an initial transient surge in TTX-resistant Na^+ current density, the density of TTX-resistant Na^+ channels in the sarcolemma decreased to about 25% of the total (see also Pappone, 1980; Caldwell & Milton, 1988). One possibility was that this was due to a transient increase in expression of TTX-resistant Na^+ channel mRNA. This was investigated using RNase protection assays.

A ^{32}P-labelled riboprobe was made to a portion of a cytoplasmic loop in the TTX-resistant Na^+ channel isoform (Rogart *et al.* 1989; Kallen, Sheng, Yang, Chen, Rogart & Barchi, 1990). The RNA probe was hybridized to total cellular RNA extracted from rat FDB muscles after various periods of denervation. As shown in Fig. 6, very little TTX-resistant Na^+ channel transcript could be detected in control innervated muscle. By 3 days after denervation, expression of this transcript was elevated more than 50-fold. Expression of the TTX-resistant Na^+ channel message decreased about 6-fold between 3 days and 3 weeks of denervation and decreased a further 5-fold by 6 weeks of denervation. These results showed that the expression of mRNA encoding the TTX-resistant Na^+ channel isoform is augmented 3 days after denervation, just as reported for the TTX-sensitive Na^+ channel (see Cooperman, Grubman, Barchi, Goodman & Mandel, 1987; Trimmer, Cooperman, Agnew & Mandel, 1990). This augmentation in transcription was transient for the TTX-resistant Na^+ channel isoform, however, and by 6 weeks of denervation the expression level of this isoform was close to that found in innervated muscle.

DISCUSSION

The main result of these experiments is the demonstration that Na^+ channel density at the endplate decreases to a level of about 60% of normal after 4–6 weeks of denervation. At the same time, the density of Na^+ channels in extrajunctional membrane increases by about 30%. This is similar to changes in the AChR density on muscle fibres following denervation (Fumagalli *et al.* 1990). Our data do not indicate whether the density would continue to decrease after longer periods of denervation or would plateau at some level close to that at 6 weeks. What is clear is that Na^+ channels remain concentrated at the endplate, even 6 weeks after maintained denervation.

Loose-patch clamp recording in the presence of TTX revealed that the TTX-resistant Na^+ channel isoform made up between 25 and 40% of the Na^+ channel population at endplates after denervation. If this TTX-resistant Na^+ channel population disappeared a long time after denervation, it would account for the decreased Na^+ channel density at long-term denervated endplates. However, results showed that both populations of Na^+ channels became reduced in density at the endplate, and

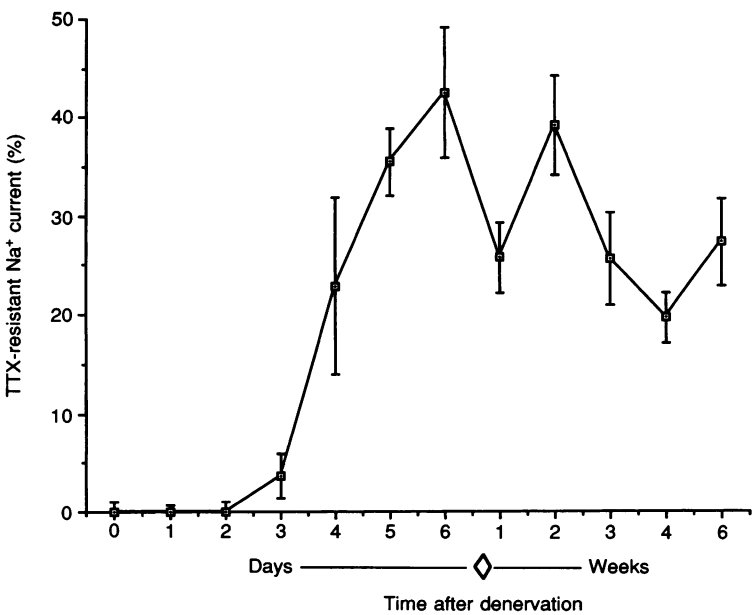

Figure 5. TTX-resistant Na^+ current at endplates following denervation

Percentage of total Na^+ current at denervated rat endplates that is contributed by TTX-resistant channels. Each point represents the mean ± S.E.M. for 10–15 fibres. Note the non-linear abscissa.

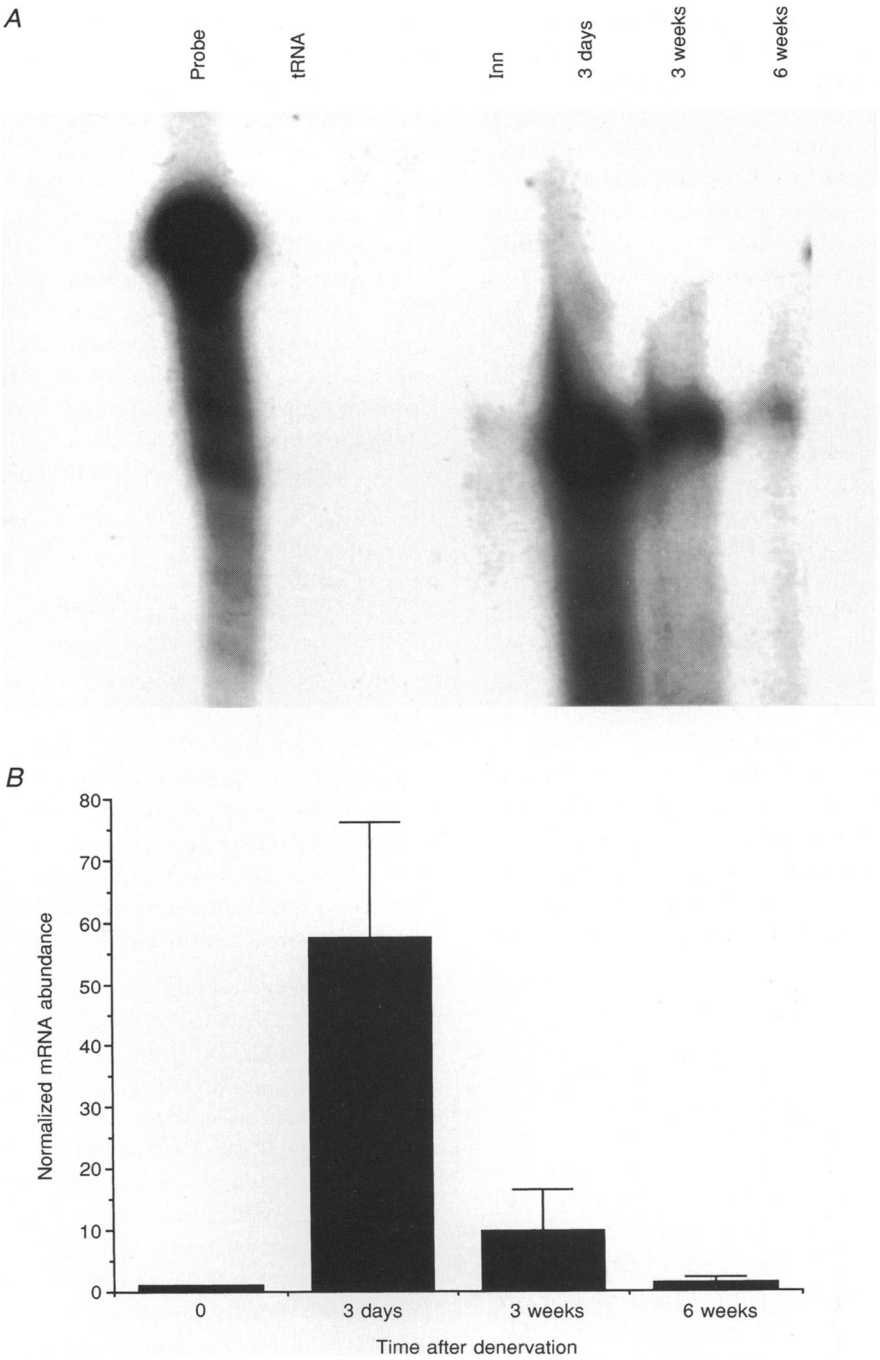

Figure 6. Detection of TTX-resistant Na^+ channel mRNA in innervated and denervated muscle

RNase protection analysis of FDB muscle total RNA samples (35 μg) from innervated rats (Inn) and from rats denervated for 3 days, 3 weeks and 6 weeks. *A*, hybridization of ^{32}P-labelled probe for the TTX-resistant Na^+ channel. The far left lane shows the probe alone. A tRNA control lane shows no signal. The autoradiograph was exposed for 6 days; the probe lane was exposed for 40 h. *B*, the percentage change for the TTX-resistant Na^+ channel message in innervated muscle (time 0) and muscle denervated for 3 days, 3 weeks and 6 weeks. Quantitation was achieved by calibrating a digital densitometric imaging program with bands obtained from RNase protection analysis of known quantities of the sense strand for the probe (see Methods). Each point is the mean of 4 measurements. Data were normalized to the maximum signal obtained for the TTX-resistant probe in innervated muscle.

the percentage of the endplate Na^+ channel population made up by TTX-resistant Na^+ channels remained at around 25% from 1 to 6 weeks after denervation. Changes in Na^+ channel distribution after long-term denervation could be due to one or more mechanisms, for example decreased synthesis or lifetime for both isoforms of the Na^+ channel, a change in the affinity of these Na^+ channel isoforms for the endplate, or loss of a molecule that maintains the synaptic Na^+ channel density.

Maintenance of Na^+ channel density at the endplate

It has been shown that postjunctional folds gradually decrease in number and depth after denervation (Matsuda *et al.* 1988). Using the loose-patch clamp technique, Ruff (1992) estimated that postsynaptic folds increase the membrane area under the pipette by approximately a factor of two. It is thus possible that the 40–50% decrease in endplate Na^+ channel density after denervation reflects not a decreased Na^+ channel density per unit membrane, but actually a decrease in the amount of membrane enclosed by the pipette at denervated neuromuscular junctions. However, two factors complicate this interpretation. (1) Matsuda *et al.* (1988) studied the peroneus longus muscle of 5- to 6-week-old male Chinese hamsters and found that junctional folds did not disappear completely, even after 8 weeks of denervation. We have no data on the postjunctional folding in our preparations, either from control muscles or after denervation. (2) Na^+ channels have been shown to be distributed non-uniformly within the postjunctional folds, with the highest density in the troughs and a decreasing concentration as one moves towards the crests of the folds (Flucher & Daniels, 1989; Boudier, Trent & Jover, 1992). Na^+ channels are absent from the crests of the folds, where AChRs are packed in a nearly crystalline array. Further experiments are required to estimate the extent of postjunctional membrane loss, and particularly the extent to which the parts of the troughs with a high density of Na^+ channels are affected. Therefore, we assume that the decreased Na^+ current reflects a change in postsynaptic folding and/or Na^+ channel density, with some Na^+ channels being labile and others stable.

The labile portion of endplate Na^+ channel density might be stabilized through the action of a secreted diffusible molecule. Several factors other than acetylcholine have recently been shown to be secreted by motor nerve terminals, including calcitonin gene-related peptide (CGRP; New & Mudge, 1986; Laufer & Changeux, 1987) and acetylcholine receptor-inducing factor (ARIA; Usdin & Fischbach, 1986; Falls, Harris, Johnson, Morgan, Corfas & Fischbach, 1990). ARIA has been shown to increase the density of Na^+ channels 2- to 4-fold on cultured myotubes (Falls *et al.* 1990; Corfas & Fischbach, 1993). The effect of CGRP on Na^+ channels has not been tested, but this neuropeptide increases the level of intracellular cAMP 4- to 5-fold (Laufer & Changeux, 1987). Elevation of intracellular cAMP increases the number of Na^+ channels in muscle cells by stimulating expression of mRNA for this protein (Catterall, 1992). Since the molecules are being secreted locally by the nerve terminal, one might expect a local stimulation of Na^+ channel RNA expression by subsynaptic nuclei. Removal of the nerve terminal after denervation might then produce a decrease in Na^+ channel expression by these nuclei. RNase protection assays indicate that expression of both Na^+ channel isoforms is transiently increased after denervation, followed by a gradual diminution in expression to approximately control levels (Fig. 6; Yang, Sladky, Kallen & Barchi, 1991). However, this technique does not provide spatial resolution of changes in RNA expression; this question would be better addressed with *in situ* hybridization.

The action of a secreted factor would have to be long lasting since there was a time lag of several weeks between removal of the factor by denervation and the reduction in endplate Na^+ channel density. This delayed redistribution of Na^+ channels might also be explained by a basal lamina or cytoskeletal molecule (see Froehner, 1991) responsible for immobilizing Na^+ channels at the endplate, that is contributed by the nerve terminal and slowly lost after denervation. Another possibility is that an increased rate of endocytosis at denervated endplates (Libelius & Tagerud, 1984) causes a loss of several membrane components, including Na^+ channels. Similar explanations have been proposed to explain the loss of junctional AChRs after long-term denervation (Fumagalli *et al.* 1990).

A linear regression analysis supported a gradual reduction in Na^+ channel density, beginning from the time of denervation (Fig. 3). However, several models could be made to fit these data. For example, examination of the means for each time point suggests that little or no change occurred in synaptic Na^+ channel density until 3 weeks of denervation, when the density decreased by about 40%. This model would imply that two mechanisms act to maintain a higher density of Na^+ channels at the endplate. One mechanism is independent of innervation, once the Na^+ channel density is established, and is responsible for about 60% of the endplate concentration of Na^+ channels. The other mechanism contributes about 40% of the total endplate Na^+ channel density and is slowly reversible after removal of innervation. This model would be consistent with results from other recent experiments studying aggregation of Na^+ channels at endplates regenerating in the absence or presence of innervation (Lupa & Caldwell, 1994). In those experiments the synaptic Na^+ channel density increased after 2 weeks of regeneration to approximately 50% of the normal level, regardless of the state of innervation. Further increase to normal adult density appeared to require innervation.

The Na^+ channel density that remains at endplates after denervation is probably controlled by a molecule stably bound to the basal lamina. One obvious candidate, the

protein agrin that acts to aggregate AChRs, was shown to have little influence on Na^+ channel distribution in adult muscle fibres in culture (Lupa & Caldwell, 1991). AChRs begin to aggregate in embryonic muscle within minutes or hours of nerve contact, while Na^+ channels begin to cluster at endplates only 1 week after birth, i.e. about 2 weeks after initial nerve contact (Lupa *et al.* 1993). Both these results suggest different mechanisms for aggregation of AChRs and Na^+ channels, implying that a molecule other than agrin may act to regulate Na^+ channel aggregation at the neuromuscular synapse. On the other hand, it is possible that agrin initiates a protracted cascade of processes that leads to synaptic maturation, one aspect of which is Na^+ channel aggregation at the neuromuscular endplate.

Expression of Na^+ channel isoform mRNA

RNase protection assays revealed an approximately 50-fold increase in expression of mRNA encoding the TTX-resistant Na^+ channel after denervation. In agreement with a previous report (Yang *et al.* 1991), this level of expression peaked about 3 days after denervation and decreased thereafter. TTX-resistant Na^+ channel mRNA transcripts were detectable, however, even after 6 weeks of denervation, indicating that expression of this isoform is a long-lasting response to removal of the nerve terminal. The level of TTX-sensitive Na^+ channel mRNA transcripts is also increased transiently after denervation followed by a slow decline in expression (see Trimmer *et al.* 1990; Yang *et al.* 1991). It is tempting to speculate that this decrease in expression of both Na^+ channel isoforms is responsible for the reduced Na^+ channel density at long-term denervated endplates. This is difficult to reconcile, however, with the finding of an increased Na^+ channel density in extrajunctional membrane.

The transient increase in expression of mRNA transcripts for the TTX-resistant Na^+ channel correlated well with the striking appearance of TTX-resistant Na^+ current after 3 days of denervation. Likewise, the gradual reduction in TTX-resistant Na^+ current density could be explained by the decrease in expression of this mRNA. The expression of transcripts for the TTX-resistant Na^+ channel thus correlated qualitatively well with changes in density of TTX-resistant Na^+ current, in both endplate and extrajunctional areas. These results are consistent with the hypothesis that TTX-resistant Na^+ channel density in the muscle cell membrane is controlled mainly at the level of mRNA transcription. On the other hand, changes in the levels of TTX-resistant Na^+ channel mRNA and Na^+ current density did not correlate quantitatively. While the level of TTX-resistant Na^+ channel mRNA found in muscles after 6 weeks of denervation was 95% less than the peak measured after 3 days of denervation, the peak of TTX-resistant Na^+ current density decreased by only ~40% between 3 days and 6 weeks of denervation. These results could be explained by an inefficient synthesis of the TTX-resistant Na^+ channel coupled with a relatively long lifetime for the channel in the muscle cell membrane. The channel lifetime is unknown in adult muscle, and the cellular signals involved in the regulation of Na^+ channel expression and distribution have yet to be identified. The results may also signal a complex regulation of the TTX-resistant Na^+ channel, both during transcription and translation. Transcriptional control of rat Na^+ channel II has been studied, and tissue-specific, negative regulatory elements were identified in the 5′ upstream region (Maue, Kraner, Goodman & Mandel, 1990). Similar studies on transcriptional regulation have not been performed for either the rat TTX-sensitive or TTX-resistant sodium channel. Denervation and the ensuing change in muscle electrical activity are important determinants of the relative expression of TTX-sensitive and TTX-resistant muscle Na^+ channels. A 5′ upstream region that confers regulation by electrical activity upon the AChR delta subunit has been reported (Chahine, Walke & Goldman, 1992). Activity-dependent regulatory elements are also likely to be present in the muscle Na^+ channel genes.

ALMERS, W., STANFIELD, P. R. & STÜHMER, W. (1983). Slow changes in currents through sodium channels in frog muscle membrane. *Journal of Physiology* **339**, 253–271.

AXELSSON, J. & THESLEFF, S. (1959). A study of supersensitivity in denervated mammalian skeletal muscle. *Journal of Physiology* **149**, 178–193.

BEAM, K. G., CALDWELL, J. H. & CAMPBELL, D. T. (1985). Na channels in skeletal muscle concentrated near the neuromuscular junction. *Nature* **313**, 588–590.

BETZ, W. J., CALDWELL, J. H. & KINNAMON, S. C. (1984). Increased sodium conductance in the synaptic region of rat skeletal muscle fibres. *Journal of Physiology* **352**, 189–202.

BOUDIER, J.-L., TRENT, T. L. & JOVER, E. (1992). Autoradiographic localization of voltage-dependent sodium channels on the mouse neuromuscular junction using ^{125}I-α-scorpion toxin. II. Sodium channel distribution on postsynaptic membranes. *Journal of Neuroscience* **12**, 454–466.

CALDWELL, J. H., CAMPBELL, D. T. & BEAM, K. G. (1986). Na channel distribution in vertebrate skeletal muscle. *Journal of General Physiology* **87**, 907–932.

CALDWELL, J. H. & MILTON, R. L. (1988). Sodium channel distribution in normal and denervated rodent and snake skeletal muscle. *Journal of Physiology* **401**, 145–161.

CATTERALL, W. A. (1992). Cellular and molecular biology of voltage-gated sodium channels. *Physiological Reviews* **72**, S15–48.

CHAHINE, K. G., WALKE, W. & GOLDMAN, D. (1992). A 102 base pair sequence of the nicotinic acetylcholine receptor delta-subunit gene confers regulation by muscle electrical activity. *Development* **115**, 213–219.

COOPERMAN, S. S., GRUBMAN, S. A., BARCHI, R. L., GOODMAN, R. H. & MANDEL, G. (1987). Modulation of sodium-channel mRNA levels in rat skeletal muscle. *Proceedings of the National Academy of Sciences of the USA* **84**, 8721–8725.

CORFAS, G. & FISCHBACH, G. D. (1993). The number of Na^+ channels in cultured chick muscle is increased by ARIA, an acetylcholine receptor-inducing activity. *Journal of Neuroscience* **13**, 2118–2125.

FALLS, D. L., HARRIS, D. A., JOHNSON, F. A., MORGAN, M. M., CORFAS, G. & FISCHBACH, G. D. (1990). M_r 42,000 ARIA: A protein that may regulate the accumulation of acetylcholine receptors at developing chick neuromuscular junctions. *Cold Spring Harbor Symposium on Quantitative Biology* LV, 397–406.

FLUCHER, B. E. & DANIELS, M. P. (1989). Distribution of Na^+ channels and ankyrin in neuromuscular junctions is complementary to that of acetylcholine receptors and the 43 kD protein. *Neuron* **3**, 163–175.

FRANK, E., GAUTVIK, K. & SOMMERSCHILD, H. (1975). Cholinergic receptors at denervated mammalian motor end-plates. *Acta Physiologica Scandinavica* **95**, 66–76.

FROEHNER, S. C. (1991). The submembrane machinery for nicotinic acetylcholine receptor clustering. *Journal of Cell Biology* **114**, 1–7.

FUMAGALLI, G., BALBI, S., CANGIANO, A. & LØMO, T. (1990). Regulation of turnover and number of acetylcholine receptors at neuromuscular junctions. *Neuron* **4**, 563–569.

KALLEN, R. G., SHENG, Z. H., YANG, J., CHEN, L., ROGART, R. B. & BARCHI, R. L. (1990). Primary structure and expression of a sodium channel characteristic of denervated and immature rat skeletal muscle. *Neuron* **4**, 233–242.

LAIRD, N. M. & WARE, J. H. (1982). Random effects model for longitudinal data. *Biometrics* **38**, 963–974.

LAUFER, R. & CHANGEUX, J. P. (1987). Calcitonin gene-related peptide elevates cyclic AMP levels in chick skeletal muscle: possible neurotrophic role for a coexisting neuronal messenger. *Journal of the European Molecular Biology Organization* **6**, 901–906.

LIBELIUS, R. & TAGERUD, S. (1984). Uptake of horseradish peroxidase in denervated skeletal muscle occurs primarily at the endplate region. *Journal of the Neurological Sciences* **66**, 273–281.

LUPA, M. T. & CALDWELL, J. H. (1991). Effect of agrin on the distribution of acetylcholine receptors and sodium channels on adult skeletal muscle fibres in culture. *Journal of Cell Biology* **115**, 765–778.

LUPA, M. T. & CALDWELL, J. H. (1994). Sodium channels aggregate at former synaptic sites in innervated and denervated regenerating muscles. *Journal of Cell Biology* **124**, 139–147.

LUPA, M. T., KRZEMIEN, D., SCHALLER, K. L. & CALDWELL, J. H. (1993). Aggregation of Na channels during development and maturation of the neuromuscular junction. *Journal of Neuroscience* **13**, 1326–1336.

MATSUDA, Y., OKI, S., KITAOKA, K., NAGANO, Y., NOJIMA, M. & DESAKI, J. (1988). Scanning electron microscopic study of denervated and reinnervated neuromuscular junction. *Muscle and Nerve* **11**, 1266–1271.

MAUE, R. A., KRANER, S. D., GOODMAN, R. H. & MANDEL, G. (1990). Neuron-specific expression of the rat brain type II sodium channel gene is directed by upstream regulatory elements. *Neuron* **4**, 223–231.

MELTON, D. A., KRIEG, P. A., REBAGLIATI, M. R., MANIATIS, T., ZINN, K. & GREEN, M. R. (1984). Efficient *in vitro* synthesis of biologically active RNA and RNA hybridization probes from plasmids containing a bacteriophage SP6 promoter. *Nucleic Acids Research* **12**, 7035–7056.

NEW, H. V. & MUDGE, A. W. (1986). Calcitonin gene-related peptide regulates muscle acetylcholine receptor synthesis. *Nature* **323**, 406–411.

PAPPONE, P. A. (1980). Voltage-clamp experiments in normal and denervated mammalian skeletal muscle fibres. *Journal of Physiology* **306**, 377–410.

REDFERN, P. & THESLEFF, S. (1971). Action potential generation in denervated rat skeletal muscle. II. The action of tetrodotoxin. *Acta Physiologica Scandinavica* **82**, 70–78.

ROBERTS, W. M. (1987). Sodium channels near end-plates and nuclei of snake skeletal muscle. *Journal of Physiology* **388**, 213–232.

ROGART, R. B., CRIBBS, L. L., MUGLIA, L. K., KEPHART, D. D. & KAISER, M. W. (1989). Molecular cloning of a putative tetrodotoxin-resistant rat heart Na^+ channel isoform. *Proceedings of the National Academy of Sciences of the USA* **86**, 8170–8174.

RUFF, R. L. (1992). Na current density at and away from endplates on rat fast- and slow-twitch skeletal muscle fibres. *American Journal of Physiology* **262**, C229–234.

SELLIN, L. C., LIBELIUS, R., LUNDQUIST, I., TÅGERUD, S. & THESLEFF, S. (1980). Membrane and biochemical alterations after denervation and during reinnervation of mouse skeletal muscle. *Acta Physiologica Scandinavica* **110**, 181–186.

SELLIN, L. C. & THESLEFF, S. (1980). Alterations in membrane electrical properties during long-term denervation of rat skeletal muscle. *Acta Physiologica Scandinavica* **108**, 243–246.

STRICKHOLM, A. (1961). Impedance of a small electrically isolated area of the muscle cell surface. *Journal of General Physiology* **44**, 1073–1088.

STÜHMER, W. & ALMERS, W. (1982). Photobleaching through glass micropipettes: sodium channels without lateral mobility in the sarcolemma of frog skeletal muscle. *Proceedings of the National Academy of Sciences of the USA* **79**, 946–950.

THESLEFF, S. & SELLIN, L. C. (1980). Denervation supersensitivity. *Trends in Neurosciences* **3**, 122–126.

TRIMMER, J., COOPERMAN, S. S., AGNEW, W. S. & MANDEL, G. (1990). Regulation of muscle sodium channel transcripts during development and in response to denervation. *Developmental Biology* **142**, 360–367.

USDIN, T. B. & FISCHBACH, G. D. (1986). Purification and characterization of a polypeptide from chick brain that promotes the accumulation of acetylcholine receptors in chick myotubes. *Journal of Cell Biology* **103**, 493–507.

YANG, J. S.-J., SLADKY, J. T., KALLEN, R. G. & BARCHI, R. L. (1991). TTX-sensitive and TTX-insensitive sodium channel mRNA transcripts are independently regulated in adult skeletal muscle after denervation. *Neuron* **7**, 421–427.

Acknowledgements

The authors would like to thank Drs A. Ribera and G. Owens for good-natured help with the RNase protection assay. Dr J. Clayton helped with the imaging of autoradiographs. This work was supported by grants from the NIH (NS-26505), the NSF (IBN-9213199), and the Muscular Dystrophy Association.

Author's present address

M. T. Lupa: Tabernash Brewing Company, 205 Denargo Market, Denver, CO 80261, USA.

Received 8 December 1993; accepted 14 July 1994.